

DIGITAL CONSERVATION OF HERITAGE BUILDINGS USING A UAV SYSTEM CONFIGURED FOR LATERAL SCANNING AND IMAGES, COMBINED WITH A HYBRID PROCESSING METHOD

Daniel ILIE^{1,2,3}, Constantin MOLDOVEANU¹, Octavian Laurentiu BALOTA^{2,4}

¹Technical University of Civil Engineering of Bucharest, 122-124 Lacul Tei Blvd, District 2, Bucharest, Romania

²Romanian Society of Photogrammetry and Remote Sensing, 124 Lacul Tei Blvd, District 2, Bucharest, Romania

³Terra Advanced Technologies SRL, 149 Bahluiului Street, Ploiesti, Romania

⁴University of Agronomic Sciences and Veterinary Medicine of Bucharest, 59 Marasti Blvd, District 1, Bucharest, Romania

Corresponding author email: danielilie17@yahoo.com

Abstract

The preservation of heritage buildings is essential in a modern society that understands the importance of architecture, culture, and history. The lack of reconstruction funds or the vision of the decision-makers can delay the realization of the works to protect these buildings. The digital conservation of these buildings can be a solution for a later reconstruction or for the creation of a realistic virtual museum. The article presents the rigorous setup and calibration of an airborne side scanner mounted on a UAV platform. Acquiring fine architectural details involves the use of more precise scanning sensors, with substantially higher costs, leading to delays. The present study shows that medium precision scanning sensors can also be used for digitizing architectural details. The side scan solution can be applied successfully in the digital preservation of buildings with a medium degree of detail, but it can also be useful in complex cases. Using optimal processing methods greatly improves the internal accuracy of the modelling with little loss in accuracy. The proposed methodology can be applied even when using superior sensors, leading to exceptional results.

Key words: digital modelling, lateral scanning, UAV, LIDAR, heritage, hybrid processing.

INTRODUCTION

Digital preservation of heritage buildings can be achieved through terrestrial scanning (Mentzer, 2021) or through image-based photogrammetric modelling. The present research paper aims to bring to the forefront a new method of achieving numerical modelling of heritage buildings. This new method involves setting up an airborne lateral scanning system and taking images for the reconstruction of historic building facades. The configuration of this system is based on an existing Unmanned Aerial Vehicle (UAV) system with vertical acquisition for optical imagery and a Light Detection and Ranging (LIDAR) sensor. To produce realistic models, a hybrid method is proposed, combining LIDAR data with images acquired from facades.

Setting up such a system will bring a degree of practical novelty, adapted to atypical situations where vertical or tilted scanning did not produce satisfactory results. The usefulness of this

system will not only be in the field of heritage buildings but also in other areas such as: monitoring of cliffs, scanning of bridges (including the lower structure), scanning of communication towers and equipment installed on them, complementing scans carried out in industrial areas, etc.

Furthermore, a hybrid method of processing the scanned LIDAR data to obtain superior digital modelling of the sensor construction parameters is presented. The purpose was to develop a methodology that, by processing medium quality data, would generate a high-quality digital model that would approximate as closely as possible the architectural details of the building. The methodology requires the creative combination of calibration methods, acquisition processes, processing methods and known software solutions.

The implementation of this innovative procedure will effectively contribute to the digital preservation of heritage buildings,

memorial houses, historical ruins, or archaeological sites.

One of the largest digital reconstructions based on LIDAR scanning was Notre-Dame Cathedral in Paris after the fire in April 2019. Terrestrial LIDAR scanning was used to preserve the lateral architectural details, ensuring high precision on the detail elements. This technology has also been used for the digital reconstruction of other heritage buildings such as the Statue of Liberty in New York, the Royal Palace in Madrid, the Opera House in Rhode Island (Development Team of Leica GeoS, 2020) or the Saigon Opera House - one of Ho Chi Minh City's most elegant and historic cultural assets (Nuron, 2021). Research using this method of reconstruction has also been carried out in Romania, the interest growing with Timișoara winning the title of European Capital of Culture in 2021 (Alionescu et al., 2019). Globally, the importance of the need to preserve heritage buildings has increased after the Paris tragedy (Buczowski, 2019), but it has always been a subject of interest for researchers (Paul-Martin, 2020).

Terrestrial scanning provides high accuracy and represents a good solution for scanning heritage buildings (Carber-White, 2021). For even higher accuracy of digital reconstruction for correlation of multiple terrestrial scans, classical geodetic methods were used (Baik et al., 2021). However, in certain situations, this method of heritage conservation has several disadvantages that can hardly be eliminated or resolved. The most well-known disadvantage arises from the fact that scanning is done from ground level, thus generating areas that are only partially scanned, these being shadowed by other architectural elements (Almukhtar et al., 2021; Boardman et al., 2018). Among the most popular technologies to eliminate these disadvantages are reconstruction from aerial imagery (Desa et al., 2021; Ehtemami et al., 2021) or LIDAR scanning reconstruction using UAV platforms (Alessandra et al., 2020; Maté-González et al., 2022). Reconstruction using aerial photogrammetric imagery often does not give a satisfactory degree of accuracy (Hu et al., 2021). Much better results have been obtained by combining various types of imagery (satellite, nadir aerial photographs, oblique or low-altitude, as well as imagery acquired from the ground) to

obtain a complex three-dimensional model (Choi et al., 2021). One of the methods used to improve accuracy is the integration of terrestrial scanning with photogrammetric modelling based on nadir or oblique aerial imagery (Alessandra et al., 2020; Costantino et al., 2021; Lerones et al., 2021).

Another method is to acquire images at the same time as aerial LIDAR scanning, thus considerably improving the geometric accuracy of the 3D model and the visual quality of the details (Development Team of Hexagon, 2020). The reconstruction of heritage buildings through this technology is done by vertical scanning and thus there are areas of the walls that are only partially scanned (Boardman et al., 2018).

In other cases, various fewer common methods have been used to eliminate these shortcomings of terrestrial laser scanning. One example is the installation of the scanner on the boom of a crane for scanning the floors of the Mores Bell Tower at various heights (Vacca et al., 2012).

Precise handheld scanners are also a solution to complement three-dimensional models obtained by terrestrial laser scanning (Ramsey, 2020). Newer technologies are LIDAR scanners based on the GeoSLAM principle (Fowkes, 2020). This operating principle has been implemented in handheld or airborne scanners which can operate both outdoors and indoors (Development Team of GeoSLAM, 2021), but have a much larger operating range than precise handheld scanners. For indoor scanning, research has also been performed in GeoSLAM scanning technology using Unmanned Ground Vehicle (UGV) (Wei et al., 2021).

Another method of scanning the 3D model of a heritage building is automated mobile (Wang et al., 2019) or pedestrian scanning with backpack-type systems (Erdal et al., 2021). In this case, some of the areas hidden behind other architectural details are scanned in detail at scanner level only.

In terms of research on side-scanners installed on UAV platforms, a lateral LIDAR system tested for scanning the interior of a forest to measure forest biomass has been identified (Hyypä et al., 2020). However, this system does not have RGB (integrated optical camera) information and has not been used in reconstructions of heritage buildings or historical sites. Another system that could also

scan sideways is Zenmuse L1, designed by DJI. This is mounted on a gimbal that can scan sideways, but its scanning accuracy is not feasible for architectural reconstructions (horizontal 10 cm @ 50 m, vertical 5 cm @ 50 m - achieved under optimal laboratory conditions) (Development Team of DJI, 2021). There are also no known applications of this system in the field of conservation of heritage buildings. Moreover, the setup of this new system is part of a whole innovative procedure for acquiring and processing LIDAR data for digital modelling of heritage building facades. The potential of LIDAR-UAV platforms is still unexploited to its true value (Kadhim et al., 2021). This is why it is necessary to deepen new methods of acquiring, processing but also configuring new systems for the reconstruction of heritage buildings or historical sites.

MATERIALS AND METHODS

1. Equipment used

The configuration of the lateral scanning system was done by physical methods, making a system to attach the reconfigured system to the drone body. The center of gravity of the scanning system was balanced with the entire UAV assembly. This new scanning system will be calibrated in terms of coordinate axis systems for each component (Global Navigation Satellite System or GNSS, LIDAR, Camera). The following equipment was used for this procedure: UAV drone DJI MATRICE M600 with LIDAR VLP 16 Puck Lite sensor, Sony α 6000 camera, CPU (central processing unit) with Inertial Measurement Unit (IMU) ADIS 16488 sensor, SPAN OEM6 receiver, DJI Dual D-RTK GNSS (rover) antennas, CHC GPS X900 (or similar) reference (base) station. Tools such as screwdrivers, calliper compasses, square with the toric level, physical coordinate axis systems, etc. were used to set up and physically calibrate the system. Software solutions used for data acquisition and processing: Phoenix Spatial Explorer, Phoenix LightHouse, Novatel Inertial Explorer, Terra Scan, Terra Match, Terra Modeler, Pix4D Mapper, Potree-Prosig, etc.

2. Test area: Little Trianon Palace

To highlight the scanning capacity of the new system, a heritage building in urgent need of

digital preservation was chosen. The Little Trianon Palace is a building in a strong state of decay, but still has many architectural elements that are well worth preserving or even restoring. Also known as the Cantacuzino Palace in Florești (Prahova County, Romania), it was designed by the famous architect Ion D. Berindey (who also designed the Cantacuzino Palace in Bucharest, the current "George Enescu" National Museum). The origin of this project is inspired by the architecture of the Petit Trianon and Grand Trianon Palaces, which are found in the gardens of the Palace of Versailles in France. The building was built in the *Mavros* style and is dominated by *rococo* and *neoclassical* architectural elements. The facades were made of white Albești limestone, where several bas-reliefs are carved. Although almost completed in 1913, this heritage building has suffered numerous destructions over the years. After the 1977 earthquake, the inner walls of the palace and its ceiling collapsed. Today only the outer walls of the palace remain, which are still witnesses of the architectural beauty.

3. Preliminary sensor calibration

In order to acquire qualitative data, the newly configured system had to be rigorously calibrated. The reference system that defines the entire assembly is the IMU coordinate system (also called the "navigation center"). For this reason, all sensors of the scanning system must be calibrated relative to the coordinate system of the IMU. The IMU sensor was mounted with X Vehicle-Left, Y Vehicle-backward and Z Vehicle-up axis relative to the UAV orientation. The first stage of the calibration involved determining the translations from the IMU to each sensor in the IMU coordinate system. Along with these translations, the rotation angles to be applied to each sensor to bring it into the IMU coordinate system were also determined. The rotations on each axis are determined in an approximate way, and in the second step they are calibrated in a rigorous way. For the determination of translations and rotations, the definition of coordinate systems for each sensor, the definition of coordinate vehicles and other auxiliary systems were considered, depending on the software applications in which the processing was performed. The preliminary calibration of the

optical sensor with respect to the IMU Body Frame is shown in Table 1

The orientation parameters of the LIDAR sensor in relation to the IMU sensor, determined in the preliminary calibration step, are centralized in Table 2. From these parameters the correction angles on each laser head were determined.

4. Calibration of the navigational system

After mounting the IMU-LIDAR-Camera sub-assembly on the UAV platform, the calibration of the navigation system was performed. Correlation of the IMU Body Frame with the coordinate system of the UAV, Vehicle Frame (X Vehicle-Right, Y Vehicle-backward and Z Vehicle-up) is necessary for processing the flight trajectory relative to the UAV orientation. Thus, to bring the aircraft into the IMU system requires a rotation around the Z-axis of 180° (direction is not relevant), the origin of the system being identical to that of the IMU. The second component of this system is the correlation of the positioning system (the two DJI Dual D-RTK GNSS antennas) by determining the translations in the Vehicle Frame system (Table 3).

The input of offsets into the data acquisition application was done in the IMU coordinate system (Spatial Explorer).

5. Precise calibration of the side scan system

Lateral scans of the three accessible facades were made with the preliminary calibrated system, as well as a vertical scan with the UAV-M600-VLP32c-SonyA7RII system. Lateral scans differ from nadir scans primarily by lower accuracy. The facade of the scanned building, as well as other obstructions that are in its vicinity, can significantly limit the satellite signal. In the present study, there were additional obstructions on all facades, which resulted in a significant decrease in the accuracy of the trajectory recorded by the GNSS antennas. A static ground calibration of the IMU sensor was performed at both the beginning and end of each flight mission. The calibration procedures of the inertial data with GNSS measurements were carried out in the air, through a straight flight line and three infinity-shaped figures (Development Team of NovAtel, 2019). Scanning was done by performing vertical scan lines at a very low speed (less than 1 m/s). In the case of vertical trajectories executed at low speed, the accuracy of the inertial data degrades rapidly. Obstructions and poor satellite data amplify this effect as the inertial sensor recalibrates with each UAV positioning.

Table 1. Preliminary calibration of the optical sensor, Sony α6000 Camera

Operation	X axis	Y axis	Z axis	RMS _x	RMS _y	RMS _z	Remarks
Offsets from Vehicle Frame -> Camera Sys.	-0.023m	0.123m	0.063m	0.002m	0.002m	0.002m	Used in post-processing (PP)
Vehicle Frame rotations -> Camera Sys.	90°	0°	180°	-	-	-	Used for OPK Export, Extrinsic Rotations X Y Z (Inertial Explorer)
Offsets from IMU Frame -> PLS Camera Sys.	-0.023m	0.063m	-0.123m	0.002m	0.002m	0.002m	Used in PP, RT, LAS Export in UTM, Extrinsic Rotations Z X Y
IMU Body Frame Rotations -> PLS Camera Sys	0°	0°	180°	-	-	-	(Spatial Explorer)

Table 2. Preliminary calibration of the VLP16 LIDAR

Operation	X axis	Y axis	Z axis	RMS _x	RMS _y	RMS _z	Remarks
Offsets from IMU -> PLS LIDAR System	-0.023m	-0.047m	0.004m	0.001m	0.001m	0.001m	Used in PP, Real-Time (RT), LAS export LAS in UTM. Extrinsic Rotations Z X Y
IMU Body Frame Rotations -> LIDAR Frame	0°	-135°	180°	-	-	-	(Spatial Explorer)

Table 3. Calibration of the Dual D-RTK GNSS system

Offsets from IMU to	X axis	Y axis	Z axis	RMS _x	RMS _y	RMS _z	Remarks
GNSS 1	-0.182m	0.021m	0.452m	0.001m	0.001m	0.001m	Used in post-processing PPK
GNSS 2	0.138m	0.021m	0.452m	0.001m	0.001m	0.001m	(Inertial Explorer)

Table 4. Calibration values of the Sony a6000 camera

Operation	X axis	Y axis	Z axis	RMS _x	RMS _y	RMS _z	Remarks
Vehicle Frame rotations -> Camera Sys. (ST70)	90.9226°	0.0648°	-179.8502°	0.0191°	0.0617°	0.0286°	Used in PP in ST70. Extrinsic Rotations X, Y, Z (Inertial Explorer)
Vehicle Frame rotations -> Camera Sys. (UTM)	90.9081°	0.0522°	-179.8581°	0.0182°	0.0617°	0.0289°	Used in PP in UTM. Extrinsic Rotations X, Y, Z (Inertial Explorer)
IMU Body Frame Rotations -> PLS Camera Sys	-0.9081°	-0.0522°	0.1419°	0.0191°	0.0617°	0.0286°	Corrections for extrinsic rotations. Used in PP, RT, LAS Export (Spatial Explorer)

Thus, the poor quality of the inertial and positioning data is also reflected in the accuracy of the trajectory, as well as in the quality of the acquired data. Consequently, it was decided to make additional calibration figures (∞) every two flightlines. However, the low accuracy of the flight path makes it necessary to identify new processing procedures to improve the accuracy of LIDAR data.

Trajectory kinematic post-processing (PPK)

To counteract the effect of satellite obstructions, the flight paths were post-processed with at least two fixed ground stations. The base network of all flights was made using the static GNSS method, to reduce the accumulation of as many errors as possible.

The post-processing kinematics of the trajectory was realised in the NovAtel Inertial Explorer application, using the best method for data processing, according to the circumstances of each flight. For trajectories with good positioning and low accuracy of the IMU data, post-processing was performed using the loosely correlated method. In case the satellite data presented multiple obstructions and the number of satellites was low, tightly correlation between GNSS and the IMU data was chosen, to obtain a trajectory estimate as close as possible to the reality. The configuration of the processing mode differed from one flight to another, depending on the context, the number of satellites, as well as their distribution.

Rigorous camera calibration

The calibration of the interior orientation parameters of the camera was carried out with the help of the PIX4D Mapper application based on a flight specially designed for this purpose on the southern facade. A hybrid calibration flight was designed, based on the principles of

calibration from classical photogrammetry, as well as from terrestrial photogrammetry taken from mobile platforms. Thus, vertical and longitudinal flight strips were made, as well as strips from a different scanning distance. Longitudinal coverage ranged from 90% to 100%, and transverse coverage was at least 60%. As a result, each tie point was identified on dozens of images helping to better calibrate the internal parameters of the camera, as well as the IMU sensor. These principles of flight realization helped to calibrate the focal length and internal orientation parameters without using control points on the building facade.

The determination of the boresight corrections on the three axes of rotation was achieved through a combined process between the PIX4D Mapper and NovAtel Inertial Explorer applications. Therefore, starting from the angles ω , ϕ , κ obtained from the Automatic Aero Triangulation (AAT) process, the angular corrections on each axis were calculated for the rigorous calibration of the optical sensor at the IMU. Since LIDAR data processing is performed in the Universal Transverse Mercator (UTM) system, it was also necessary to calibrate the camera in this coordinate system for points fusion with the optical data. The rigorous calibration of the camera in relation to the IMU sensor was carried out both in the UTM system and in the Stereographic 1970 system, with small differences in the angles ω , ϕ , κ depending on the coordinate system used. The calibrated values of the initial rotations (Table 1) are centralized in Table 4.

Following the calibration, the angular errors on the three external orientation angles of the images decreased significantly compared to the initial errors (Figure 1).

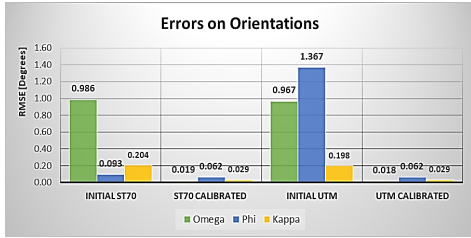


Figure 1. External Orientation Errors - before and after camera calibration with respect to the IMU sensor

After calibration, the LIDAR data was exported in LAS format (UTM system) for rigorous calibration in the TerraScan and TerraMatch applications, respectively. The transformation of LIDAR data into the national systems of Romania (Stereographic 1970) was realised at the final stage, due to considerations related to accuracy and the software applications used.

Rigorous calibration of laser heads

Correction angles on each laser head were determined using the TerraMatch application. To be able to perform the calibration, a hybrid calibration method was used, using both principles from the calibration of aerial scans and from mobile (terrestrial) scans. To calibrate the correction angles for each laser head it was decided to use two perpendicular facades as in the case of mobile scans. But with lateral scans, horizontal surfaces (such as the ground surface) are affected by much larger errors due to the large incident scan angles. Additionally, hard horizontal surfaces are required for mobile scanner calibrations. In the present study there are no such surfaces, the land around the palace being lawn type. Therefore, a hybrid way of calibration was identified, using the facades of two perpendicular walls, but also the horizontal surfaces, as well as the inclined ones that are part of these facades (sills, windowsills, beams, ceilings, columns, etc.).

Scans made on the southern and eastern facade were used. A total of 12 vertical strips, 3 detail strips and one horizontal strip on each side were used.

The LIDAR points were classified by object classes for each strip and for each laser head (16 heads). The facades that were used in the calibration of the LIDAR heads were classified in a separate class of objects. The calibration was made based on the corresponding lines (tie

lines) identified on each strip, generated by the 16 laser heads.

The TerraMatch application was not designed for calibrations based on side scans. However, if one forces the parameterization contrary to the user manual, very good results can be obtained. Normally, horizontal lines (perpendicular or along the flight) as well as lines of constant slope are searched on the ground class, where in theory there must be scans of hard surfaces (roads, platforms). In the current study there is no such class on which to generate reliable results. Consequently, the application was forced to identify the corresponding horizontal and oblique lines in the object class in which the two facades were classified. More than six thousand sections of corresponding lines were identified between the laser data of each head, in the coverage areas. The lines identified on the south facade, as well as working process in TerraMatch, are exemplified in Figure 2.

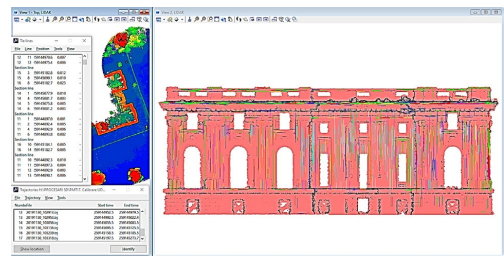


Figure 2. Identifying the corresponding tie lines on the Southern facade - TerraMatch

The length of the sections where the corresponding lines were searched was established according to the average density of points on the facades, generated by each individual laser head. Therefore, corresponding lines were searched in sections that varied from 0.8 m to 5.0 m. Using the corresponding lines from each section, but also the post-processed flight paths, the three correction angles on each laser head were determined (Figure 3).

In order for the obtained data to be reliable, corresponding lines that have a direct impact (on their direction) in solving each angle (yaw, pitch, roll) must be used. Another important point is that this calibration does not adjust the flight bands to each other. By calibrating the laser heads, only the internal accuracy on each band is improved. This is an internal strips calibration and not a calibration between strips.

Theoretically, through this type of calibration, we want to get as close as possible to the internal accuracy of the sensor used, VLP16 (± 3 cm) on each strip (Development Team of Velodyne, 2016). In order to obtain qualitative data for the preservation of the architectural details, in the next step the LIDAR strips will be calibrated, using the data corrected with the angular values from Figure 3.

	Translation X/right	Translation Y/up	Translation Z/rear	Rotation X/pitch	Rotation Y/yaw	Rotation Z/roll	Rotation
1	0.000 m	0.000 m	0.000 m	0.1358 °	0.0259 °	-0.0319 °	0.14°
2	0.000 m	0.000 m	0.000 m	0.0921 °	-0.0488 °	0.0099 °	0.10°
3	0.000 m	0.000 m	0.000 m	0.1810 °	0.0100 °	-0.1262 °	0.22°
4	0.000 m	0.000 m	0.000 m	0.0982 °	-0.0134 °	0.0154 °	0.10°
5	0.000 m	0.000 m	0.000 m	0.1236 °	-0.0072 °	-0.0212 °	0.13°
6	0.000 m	0.000 m	0.000 m	0.0990 °	-0.0347 °	0.0039 °	0.10°
7	0.000 m	0.000 m	0.000 m	0.1233 °	-0.0194 °	-0.0214 °	0.13°
8	0.000 m	0.000 m	0.000 m	0.1131 °	-0.0268 °	0.0059 °	0.12°
9	0.000 m	0.000 m	0.000 m	0.1199 °	-0.0178 °	-0.0177 °	0.11°
10	0.000 m	0.000 m	0.000 m	0.0919 °	-0.0189 °	0.0033 °	0.09°
11	0.000 m	0.000 m	0.000 m	0.1200 °	-0.0232 °	-0.0121 °	0.13°
12	0.000 m	0.000 m	0.000 m	0.0904 °	-0.0343 °	0.0024 °	0.10°
13	0.000 m	0.000 m	0.000 m	0.1008 °	-0.0041 °	0.0103 °	0.10°
14	0.000 m	0.000 m	0.000 m	0.0965 °	-0.0097 °	0.0035 °	0.10°
15	0.000 m	0.000 m	0.000 m	0.0939 °	-0.0356 °	0.0081 °	0.10°
16	0.000 m	0.000 m	0.000 m	0.1119 °	-0.0216 °	0.0052 °	0.11°

Figure 3. Applying determined corrections for each laser head - Phoenix Spatial Explorer

6. Hybrid procedure for side scan processing

As previously shown, the quality of side scans is much lower than that of nadir scans. To improve the quality of the scanned data, it is necessary to perform a data calibration based on correlation algorithms. As in the case of the calibration of the laser heads, the corresponding lines will be used to calibrate the LIDAR strips. This time the corresponding lines are searched between the strips and will be used for angular corrections, but also for fine positioning corrections (determined by fluctuating positioning errors of the trajectory).

Correction of systematic errors

In the case of lateral LIDAR scans, the systematic errors are defined by angular rotations (*yaw*, *pitch*, *roll*) and three-dimensional translations (*north*, *east*, *elevation*) which are constant on each scan strip. In Figure 4 a cross-section on the western facade is exemplified where the influence of systematic errors can be seen (the points in the section have different colours for each overlapping strips). Corresponding lines were searched for each strip separately, using all the data from the 16 laser heads. Therefore, the point density is very high compared to the previous calibration procedure.

In this context, the search sections of the corresponding lines varied between 0.4 m and 5.0 m. As with the laser heads, horizontal and inclined lines were also searched on the facades, being the only hard surfaces in this case study. To limit errors due to the incident scanning angle, the LIDAR data were filtered at an angle of 80° , perpendicular to the scanning direction (building facades). The inconsistency between scan bands is generated equally by the poor quality of positioning and attitude. Therefore, an iterative method for block determination of angular rotations (*yaw*, *pitch*, *roll*) and of three-dimensional translations (*north*, *east*, *elevation*), related to each scan strip will be addressed.

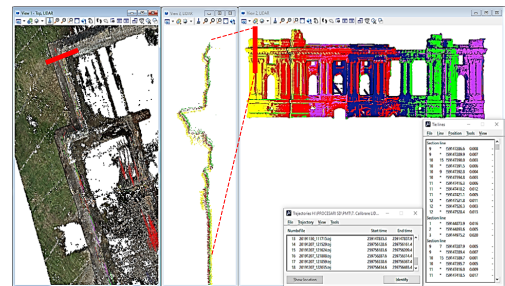


Figure 4. Calibration of LIDAR data on strips using only building facades - TerraMatch

Systematic error calibration was performed on all three facades in two iterations, using over 2500 sections in each iteration. After determining the corrections in iteration 1, they were applied to each individual strip. After applying the corrections, the quality of the LIDAR data was verified by survey with the help of cross-sections, but also with the help of statistical reports on the average magnitude on the data of the building facades (0.043 m). In the second iteration, the process of identifying the corresponding lines between the strips was resumed on the corrected data set. After determining and applying systematic corrections (significantly smaller in this iteration) an average magnitude of 0.031 m was obtained. This value is very close to the theoretical scanning capability of the VLP16 sensor (± 3 cm), which is why another iteration would not significantly improve the internal accuracy of the LIDAR data.

Correction of random errors

Visual verification of LIDAR data through cross-sections and longitudinal sections is absolutely necessary and cannot be replaced by statistical reports generated by processing applications (TerraMatch in this case). Random errors can hide behind a statistical report that appears to confirm the high quality of a dataset. In the case of the present study, under the circumstances outlined above, it is erroneous to assume that the scan strips are not also affected by significant random errors in some areas. Following visual checks, several such areas were identified, which confirmed the above hypothesis. As in the case of data strip calibration, random errors were considered to be caused by angular rotations (*yaw, pitch, roll*) as well as three-dimensional translations (*north, east, elevation*), affecting small portions or in different proportions a LIDAR data strip.

To correct these random errors, the procedure described above was used, but using small working sections (between 0.3 m and 1.5 m). Their density was much higher than in the previous cases, searching for corresponding lines at distances of up to 0.1 m between them. The underlying principle is to cover the entire scanning duration with corresponding lines. Corrections can therefore be calculated for each scanning second, in relation to the time position on the scan line. Since calibration processes are themselves affected by errors in identifying correlation lines, it was considered that a correct application is one that is also correlated with the a priori flight trajectory accuracy determined for each second. Therefore, the identified corrections were weighted according to the trajectory errors at that time position (Figure 5).

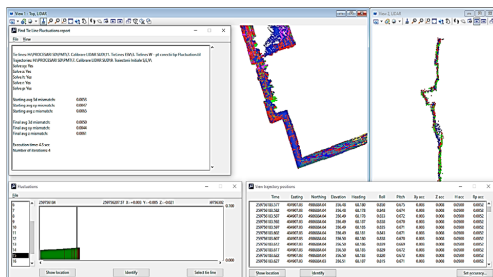


Figure 5. Determination and application of random errors in correlation with flight trajectory accuracy, TerraMatch

More than 7000 sections with corresponding lines were used to determine random corrections. In most cases, the position corrections were in the order of millimetres. Following the visual checks undertaken, no further random errors were identified on the facades of the Little Trianon Palace. However, the average amplitude remains around 3 cm.

Improvement of lateral scanning accuracy

Even if the data has been calibrated close to the maximum scanning potential of the LIDAR sensor, a dispersion of about ± 3 cm is not desirable when scanning architectural details such as stucco, bas-reliefs, blazons, pattern columns, etc. In this case, the theoretically best solution is to use a scanning sensor with a much higher internal accuracy. But this is not always feasible, mainly because of high costs.

At the end of the calibration procedure, it is proposed to improve the internal accuracy of the current data.

With accurately calibrated data, but also with a very high density of points (over 90 points/dm²), it is possible to use the average of the dispersion over the scanned area. Three-dimensional segmentation based on a value that fits the magnitude of the data and does not affect the scanned details is used to make this adjustment. The adjustment of the maximum magnitude of the data was performed iteratively, using a 6 cm segmentation and then a 3 cm segmentation. Thus, the internal accuracy of the scanning performed was optimised to 5-10 mm, with little loss of data accuracy. Surface averaging requires LIDAR data free of noise points and well calibrated between strips.

In areas affected by such errors, surface averaging improves the internal accuracy of the LIDAR data but can also leave noise points behind. This can be removed by a statistical filtering algorithm in TerraScan.

Figure 6 shows a section on the eastern facade with the sequential calibration between strips 5, 6 and 7.

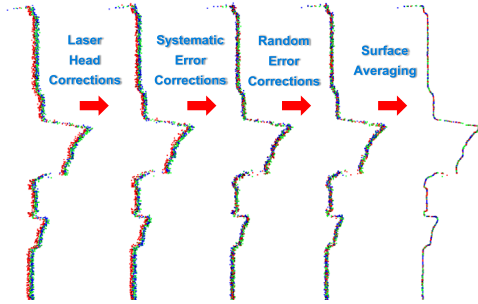


Figure 6. Example of sequential calibration performed between strips 5, 6, 7 (East)

The quality of the final data is also highlighted in Figure 7 using the visualization in the Potree-Prosig application (Schuetz, 2016).



Figure 7. Viewing calibrated LIDAR data in the Potree-Prosig web application

The aim of this research is to highlight the quality optimizations that can be achieved by various processing methods. This does not mean that fine architectural details can be reconstructed by average quality sensors. The recommendation is that scans should be performed with sensors of the highest accuracy, which through calibration and processing can produce truly stunning results.

RESULTS AND DISCUSSIONS

1. Digital model of the Little Trianon Palace

In order to obtain the digital model of the scanned facades, the final data was filtered for vegetation near the facades as well as vegetation growing on the walls or in the window area. The LIDAR scan was also filtered by the supporting scaffolding of degraded columns on the west side of the ruins (Figure 8). The digital model of the facades was classified into a separate object class for ease of use.

2. Integration of lateral and vertical scans

In order to have a complete model of the ruins of the Little Trianon Palace, the lateral scan was enriched with data from the nadir scan. The completion was done for the inner areas of the ruin and for the upper parts where the data from the lateral scans were insufficient. The ground control points (base network), the post-processed trajectory and the rigorous calibration ensured the accuracy required to combine the two data sets. The selection of data from the vertical flight was performed with the TerraScan application, using selection procedures in the vertical plane as well as on sections. The final digital model was highlighted with the Potree-Prosig web application in Figure 9.

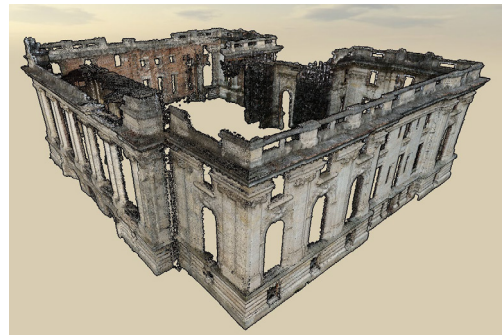


Figure 8. The digital model of the facades - visualization in the Potree-Prosig web application



Figure 9. The complete digital model of the Little Trianon Palace - Potree-Prosig visualization

In the end, the data were accurately transformed into national coordinate systems using RoTLAS APP v1.62 (Ilie et al., 2022). The accurate model transformation can be useful in the design and execution of the rehabilitation of this heritage building.

3. Creating the realistic 3D model

The flights performed did not have the primary purpose of three-dimensional modelling based on the images taken. However, the images taken laterally can be combined with those taken nadir to obtain a realistic 3D model.

Realistic modelling based on optical data

The following data were used to obtain this model: calibrated interior orientation parameters and exterior orientation data with corrected rotation angles in national coordinate systems. The application used for the realistic modelling of the whole Little Trianon Palace was PIX4D Mapper. It generates optimal results that can be used later in various digital projects such as those based on virtual reality (VR), digital twins or augmented reality (AR). The model obtained preserves quite a lot of the architectural details of the facades (Figure 10), but for precision details it is necessary to use another software solution.



Figure 10. 3D modelling of the Little Trianon Palace based on lateral and vertical images - PIX4D Mapper

However, quite a lot of errors are found in the mesh surface, in areas with noise points. The result can be improved by a manual and laborious filtering of the points in the dense cloud. Using LIDAR scans in combination with optical data can bring more accuracy for realistic modelling.

For the finest modelling, the 3DF Zephyr software solution was used. This application generates qualitative results using only images, as can be seen from the 3D bas-relief generated on the Eastern facade shown in Figure 11.



Figure 11. 3D detail of the bas-relief of the Eastern gate - image based model - 3DF Zephyr

Hybrid modelling of the heritage building

In order to eliminate the deficiencies generated by three-dimensional image-based models (scale errors, noise points, non-conforming textures, voids, etc.) a hybrid modelling based on LIDAR data was chosen. Using the imagery taken on the southern facade, the reconstruction of the model was performed. The dense cloud was aligned and scaled to the LIDAR cloud, calibrated and transformed to national coordinate systems. This georeferencing helped to correlate the images with the LIDAR point cloud. Finally, a qualitative three-dimensional model was produced using the LIDAR data and the images correlated with it (Figure 12).



Figure 12. Hybrid 3D model - LIDAR and optical data - 3DF Zephyr

For a rigorous analysis of the obtained hybrid model, it was compared with the classical realistic model obtained from the images and the dense point cloud. A detailed comparison is

shown on the bas-relief on the south facade in Figure 13.



Figure 13. Modelling the bas-relief on the southern facade: based on images (left) and based on LIDAR and Images (right) - 3DF Zephyr

This application is an excellent solution for realistic qualitative models, optical or hybrid generated. Although the application is optimized for big data management, the major disadvantage is that 3D models cannot be easily used in generic visualization applications due to the huge amount of data.

CONCLUSIONS

Scanning fine architectural details involves using the most accurate scanning sensors possible. High accuracy usually brings with it substantially higher costs, so the digitisation of heritage buildings is often delayed. This study has shown that medium accuracy scanning sensors can also be used to preserve architectural details through digitisation. The lateral scanning solution can be successfully used in the digital reconstruction of buildings with a medium degree of detail (such as memorial houses) but can also be useful in more complex cases. The solution does not offer the quality of a high-precision sensor, but optimal processing methods greatly improve the internal accuracy of the modelling, with little loss of accuracy. Therefore, the proposed methodology can be applied even when using superior sensors, leading to exceptional results.

Rigorous calibration of a side scanning system is essential and increases data accuracy. Systematic errors and most of the random errors can be corrected by correlation methods between scanning strips. Most of the time this process is iterative and requires a lot of processing time. Consequently, it is desirable to avoid the accumulation of such errors by using the best LIDAR data acquisition procedures. This is not always possible, which is why the

proposed hybrid method for calibration and processing is an optimal solution.

Surface averaging by segmentation must be done with caution so not to lose too much of the accuracy of the scanned shapes. Using it at the same time as preserving fine detail can lead to noise points in certain areas of the scan.

Calibration of the optical sensor to the IMU, and calibration of the LIDAR to the IMU, are essential to obtain LIDAR data with correct RGB information. Calibration of LIDAR data is necessary if hybrid 3D modelling desired.

Digital models are much easier to visualise and to use than realistic 3D models. Three-dimensional realistic models can be produced using both side images and a combination of LIDAR and optical data. The quality of the models produced by the two methods is approximately similar (Figure 13), but an increase in the quality of detail is observed in the image-based model. It should be noted that this accuracy was also ensured due to the very high resolution of the images (the pixel on the building facade being of the order of 3-5 mm). Moreover, the quality of the image pattern is determined by the use of images with a longitudinal coverage of about 90%. In the context of images with lower coverage, the quality of the resulting model would be poorer and would include shape and scale deformations. Therefore, the use of a hybrid method is a very correct option to generate 3D models. In this sense, the LIDAR data cloud can be used for scaling and constraining the dense point cloud or it can be used to make the digital twin models (Ćosović et al., 2022). The digital model of the Little Trianon Palace has been made available to the private owner via the Potree-Prosig web application. This will be launched on the official website to offer the possibility of virtual tours of the Little Trianon Palace or to implement a digital twin model.

Even though the internal accuracy of the LIDAR sensor is not very suitable for scanning heritage buildings with complex architectural details, the side scanner can be useful in many other types of work. These include scanning sea cliffs, scanning surface mining operations, scanning bridge infrastructure, scanning towers or power poles, etc. The boresight camera calibration and the LIDAR sensor calibration, both performed in relation to the IMU, determine a calibration

between the two acquisition sensors as well. As a result, LIDAR data can be accurately fused with optical data. Hybrid methods of calibrating and enhancing LIDAR data can also be successfully applied to mobile scans.

The calibration and configuration of this system opens up similar new research opportunities. In this regard, the configuration of a shore scanning system that can be used from a boat or an autonomous system is being considered.

ACKNOWLEDGEMENTS

The applications used were provided by Tehnognis Grup SRL, Prosig Expert SRL and the Technical University of Civil Engineering of Bucharest. A demo license was used for 3DF Zephyr. Finally, we thank to all those who directly or indirectly supported this research.

REFERENCES

- Alessandra, C., Antonino, M., Mirko, S., & Domenica, C. (2020). *Integration of terrestrial laser scanning and UAV-SFM technique to generate a detailed 3D textured model of a heritage building*. Paper presented at the Proc.SPIE.
- Alionescu, A., Herban, S., & Vilceanu, C. B. (2019). *3D modelling of cultural heritage objective in Timisoara using precise LiDAR* (Vol. 2116).
- Almukhtar, A., Saeed, Z. O., & Tah, H. A. a. J. H. M. (2021). Reality Capture of Buildings Using 3D Laser Scanners. *MDPI, CivilEng*. doi:10.3390/civileng2010012
- Baik, A., Almaimani, A., Al-Amodi, M., & Rahaman, K. R. (2021). Applying digital methods for documenting heritage building in Old Jeddah: A case study of Hazzazi House. *Digital Applications in Archaeology and Cultural Heritage*, 21, e00189. doi:https://doi.org/10.1016/j.daach.2021.e00189
- Boardman, C., Bryan, P., McDougall, L., Reuter, T., Payne, E., Moitinho, V., Rodgers, T., Honkova, J., O'Connor, L., Blockley, C., Andrews, D., Bedford, J., Sawdon, S., Hook, L., Green, R., Price, K., Klÿn, N., & Abbott, M. (2018). *3D Laser Scanning for Heritage. Advice and Guidance on the Use of Laser Scanning in Archaeology and Architecture*.
- Buczowski, A. (2019). *How the tragic fire at Notre Dame will accelerate the adoption of laser scanning of historic architecture*. Retrieved from https://geoawesomeness.com/how-the-tragic-fire-at-notre-dame-will-accelerate-the-adoption-of-laser-scanning-of-historic-architecture/
- Carber-White, K. (2021). 3D Scanning Technology Plays Key Role in Historic Preservation Project. Retrieved from https://www.directionsmag.com/article/10645
- Choi, Y., Yang, Y.-J., & Sohn, H.-G. (2021). Resilient cultural heritage through digital cultural heritage cube: Two cases in South Korea. *Journal of Cultural Heritage*, 48. doi:10.1016/j.culher.2021.01.007
- Ćosović, M., & Maksimović, M. (2022). Application of the digital twin concept in cultural heritage. *VIPERC2022: 1st International Virtual Conference on Visual Pattern Extraction and Recognition for Cultural Heritage Understanding*.
- Costantino, D., Pepe, M., & Restuccia, A. G. (2021). Scan-to-HBIM for conservation and preservation of Cultural Heritage building: the case study of San Nicola in Montedoro church (Italy). *Applied Geomatics*. doi:10.1007/s12518-021-00359-2
- Desa, H., Azizan, M. A., Zulkepli, N. N., & Romeli, N. (2021). Heritage Building Modelling: Photogrammetry Challenges in Producing an As Built Drawing (ABD) Using Unmanned Aerial System (UAS). *Atlantis Press, Journal of Robotics, Networking and Artificial Life*. doi:10.2991/jrma.lk.201215.003
- Development Team of DJI. (2021, 05.2021). *ZENMUSE L1 User Manual*. User Manual. China.
- Development Team of GeoSLAM. (2021). *Meet the ZEB Horizon: The Ultimate Mobile Mapping Tool*. Retrieved from https://geoslam.com/solutions/zeb-horizon/
- Development Team of Hexagon. (2020). Reporter - Geosystems Division. *REPORTER*, 88.
- Development Team of Leica GeoS. (2020,19.07.2020). The Vital Role of Laser Scanning in Heritage Conservation. *Survey & Construction Technology*. Retrieved from https://globalsurvey.co.nz/surveying-gis-news/the-vital-role-of-laser-scanning-in-heritage-conservation/
- Development Team of NovAtel. (2019). Waypoint Products Group - A NovAtel Precise Positioning Product [User Manual v8.80]: Hexagon, NovAtel Inc.
- Development Team of Velodyne. (2016). Velodyne LIDAR Puck Light - Light weight real-time 3D LiDAR sensor. Retrieved from https://velodynelidar.com/wp-content/uploads/2019/12/63-9378_Rev-F_Ultra-Puck_Datasheet_Web.pdf
- Ehtemami, A., Park, S., Bernadin, S., Lescop, L., & Chin, A. (2021). Review of Visualizing Historical Architectural Knowledge through Virtual Reality. *HAL*.
- Erdal, K., & Makineci, H. (2021). Documentation of Cultural Heritage with Backpack Lidar Usage on Photogrammetric Purpose. *Turkey Lidar Journal*. doi:10.51946/melid.921032
- Fowkes, D. (2020). Bringing the past to life: 3D mapping historic sites for restoration. Retrieved from https://www.pbctoday.co.uk/news/bim-news/historic-sites-mapping/78863/
- Hu, Y., Chen, X., Tang, Z., Yu, J., Chen, Y., Wu, Z., Yang, D., & Chen, Y. (2021). Collaborative 3D real modeling by multi-view images photogrammetry and laser scanning: The case study of Tangwei Village, China. *Digital Applications in Archaeology and Cultural Heritage*, 21, e00185. doi:https://doi.org/10.1016/j.daach.2021.e00185
- Hyypää, E., Hyypää, J., Hakala, T., Kukko, A., Wulder, M. A., White, J. C., Pyörälä, J., Yu, X., Wang, Y.,

- Virtanen, J.-P., Pohjavirta, O., Liang, X., Holopainen, M., & Kaartinen, H. (2020). Under-canopy UAV laser scanning for accurate forest field measurements. *ISPRS Journal of Photogrammetry and Remote Sensing*, 164, 41-60. doi:<https://doi.org/10.1016/j.isprsjprs.2020.03.021>
- Ilie, D., Balotă, O. L., Iordan, D., & Nicoară, P. S. (2022). Algorithm and application development for precise and accurate transformation of LIDAR point clouds into national coordinate systems of Romania using official equations and quasigeoid model. *ISPRS Ann. Photogramm. Remote Sens. Spatial Inf. Sci.*, V-4-2022, 181-188. doi:10.5194/isprs-annals-V-4-2022-181-2022
- Kadhim, I., & Abed, F. M. (2021). The Potential of LiDAR and UAV-Photogrammetric Data Analysis to Interpret Archaeological Sites: A Case Study of Chun Castle in South-West England. *ISPRS - International Journal of Geo-Information*.
- Lerones, P. M., David Olmedo, Ana López-Vidal, Gómez-García-Bermejo, J., & Zalama, E. (2021). BIM Supported Surveying and Imaging Combination for Heritage Conservation. *MDPI, Remote Sensing*. doi:10.3390/rs13081584
- Maté-González, M. Á., Di Pietra, V., & Piras, M. (2022). Evaluation of Different LiDAR Technologies for the Documentation of Forgotten Cultural Heritage under Forest Environments. 22(16), 6314.
- Mentzer, R. (2021). 3D Scans Will Allow Historic Building Slated For Demolition To Be Rebuilt In Virtual Reality. Retrieved from <https://www.wpr.org/3d-scans-will-allow-historic-building-slanted-demolition-be-rebuilt-virtual-reality>
- Nuron, H. M. (2021). Heritage-BIM model to future proof an Opera House. Retrieved from <https://leica-geosystems.com/case-studies/reality-capture/heritage-bim-model-to-future-proof-an-opera-house>
- Paul-Martin, R. (2020,1.07.2020). Preserving our world's heritage with advanced laser scanning. Retrieved from <https://hxgnspotlight.com/preserving-worlds-heritage-advanced-laser-scanning/>
- Ramsey, D. (2020). Using 3D Scanning for Heritage Preservation. 3D Scanning. Retrieved from <https://blog.trimech.com/using-3d-scanning-for-heritage-preservation>
- Schuetz, M. (2016). *Potree: Rendering Large Point Clouds in Web Browsers* (Engineer Bachelor Thesis), Vienna University of Technology, Vienna. (0825723)
- Vacca, G., Deidda, M., Dessi, A., & Marras, M. (2012). Laser scanner survey to cultural heritage conservation and restoration. *ISPRS - International Archives of the Photogrammetry, Remote Sensing and Spatial Information Sciences*, XXXIX-B5, 589-594. doi:10.5194/isprsarchives-XXXIX-B5-589-2012
- Wang, Y., Chen, Q., Zhu, Q., Liu, L., Li, C., & Zheng, D. (2019). A Survey of Mobile Laser Scanning Applications and Key Techniques over Urban Areas. *Remote Sensing*.
- Wei, W., Shirinzadeh, B., Nowell, R., Ghafarian, M., Ammar, M. M. A., & Shen, T. (2021). Enhancing Solid State LiDAR Mapping with a 2D Spinning LiDAR in Urban Scenario SLAM on Ground Vehicles. *MDPI, Sensors*. doi:10.3390/s21051773